Biochimica et Biophysica Acta 1828 (2013) 1683–1689

Contents lists available at SciVerse ScienceDirect

Biochimica et Biophysica Acta

journal homepage: www.elsevier.com/locate/bbamem

Connected and isolated CH_2 populations in acyl chains and its relation to pockets of confined water in lipid membranes as observed by FTIR spectrometry

E.A. Disalvo *, A.M. Bouchet, M.A. Frias

Laboratory of Biointerphases and Biomimetics Systems, CITSE (Universidad Nacional de Santiago del Estero, and CONICET), RN 9, Km 1125, 4206 Santiago del Estero, Argentina

ARTICLE INFO

Article history:
Received 12 October 2012
Received in revised form 15 January 2013
Accepted 13 February 2013
Available online 13 March 2013

Keywords:
Lipid membrane
Water pocket
FTIR
Methylene stretching mode
Water band
Phase transition

ABSTRACT

Analysis of the band corresponding to the frequency of vibrational symmetric stretching mode of methylene groups in the lipid acyl chains and the bands of water below and above the phase transition of different lipids by Fourier transform infrared spectroscopy gives strong support to the formation of confined water pockets in between the lipid acyl chains. Our measures and analysis consolidate the mechanism early proposed by Traüble, in the sense that water is present in kinks formed by trans-gauche isomers along the hydrocarbon tails. The formation of these regions depends on the acyl lipid composition, which determines the presence of different populations of water species, characterized by its degree of H bond coordination in fluid saturated or unsaturated lipids. The free energy excess due to the reinforcement of the water structure along few water molecules in the adjacencies of exposed membrane residues near the phase transition is a reasonable base to explain the insertion and translocation of polar peptides and aminoacid residues through the biomembrane on thermodynamic and structural grounds.

1. Introduction

Presence of water in the membrane structure has been recently invoked to interpret the insertion of highly hydrophilic aminoacid moieties in pools between acyl chains, described as water pockets [1]. Penetration of amphipathic helices into the hydrophobic interior of phospholipid membranes has been explained by a mechanism denoted as "snorkeling". The "snorkel effect" of positively charged aminoacids, such as lysine or arginine, is favored by the long hydrocarbon side chains that may penetrate deeper into the acyl chain region. The high positively charged guanidinium group can only enter the membrane provided water domains are present or formed as a consequence of the aminoacid interaction with membrane groups [2–4].

The possibility that stationary water can be present in lipid membranes, was previously postulated by Traüble [5]. In this proposal, water can diffuse across the lipid membrane by jumping from hole to hole in the lipid matrix. These holes were formed by fluctuations of the acyl chain trans-gauche isomers denoted as kinks. Each water molecule, according to Traüble, can occupy a kink of the molecular dimension of a CH_2 vacant.

This visualization was accepted years ago, and several permeability models had taken advantage of it to explain the diffusivity of water molecules across the lipid bilayers. In this regard, kinks were much easier to be formed above the phase transition than below, explaining the sudden increase in water permeation in the fluid state in comparison with the gel state. The kink formation was induced by the head group conformational changes triggering the propagation of kinks along the acyl chains and hence, the diffusion of water [6].

In this context, the recent studies of amino acid penetration recall in some extent these ideas. However, kink formation or condensation is not cited and an apparently a new ¨structural¨ feature, such as pockets, is introduced. In addition, neither structural nor thermodynamic correlations with the lipid and the water states have been done so far.

The admittance that water is buried in phospholipid membranes suggests that it would be facing the lipid head groups and apolar alkyl chains [7] In this regard, it has been experimentally demonstrated that water may penetrate the lipid bilayer reaching a plane located at the region of the carbonyl groups [8,9]. This penetration changes the dielectric properties of the lipid membranes [10].

In addition, it is well known that at the phase transition a reduction of the membrane thickness and area per lipid increase is accomplished as determined by SAXS [11]. Above this transition, lipid membranes reach the higher disorder state due to the increase in the trans-gauche isomers in the lipid acyl chains [12]. Parallel to this increase in chain mobility, the water amount in the bilayer increases from 7 to 20 water molecules per lipid in the case of phosphatidylcholines and from 4 to 7 in phosphatidylethanolamines with a slight variation with the chain length [13].

Differential scanning calorimetry provides the total enthalpy change of the phase transition that can be interpreted in terms of the

* Corresponding author. Tel.: +54 11 1551752977.
E-mail address: disalvoanibal@yahoo.com.ar (E.A. Disalvo).

0005-2736/$ – see front matter © 2013 Published by Elsevier B.V.
http://dx.doi.org/10.1016/j.bbamem.2013.02.007

cooperative units of the molecules contributed by the acyl chain residues [14]. In this condition, other experimental results, such as the decrease of the dipole potential in monolayers, suggest concomitant changes in water organization [15]. More indirectly, changes in turbidity or refractive index may be also interpreted as related to changes in the membrane density due to water penetration [16,17].

On the other hand, the state of water at different lipid phase states has been indirectly determined by fluorescence anisotropy methods, using probes inserted in different regions of the bilayer. The steep decrease in order parameter at the phase transition is accompanied by an increase in polarity as shown by fluorescence measures using Laurdan as a probe located at the membrane interphase [18]. The generalized polarization (GP) in the gel state is 0.6–0.7 and −0.1 and 0.2 above T_c for dimyristoylphosphatidylcholine (DMPC) and dimyristoylphosphatidylethanolamine (DMPE), respectively. GP values are related with the number and motional freedom of the water molecules around the fluorescent probe, assumed to reflect indirectly the state of the lipid environment. These changes in polarity have been ascribed to an increase of water in the membrane phase [18].

Although the mechanism proposed by Traüble was widely accepted, no direct experimental evidences of the simultaneous change in the CH_2 kink state and water have been offered. The method that provides a visualization of the membrane state at the molecular level, both of lipids and water, is FTIR spectroscopy. In adequate conditions, it provides a direct measure of the acyl chain state simultaneous with the water state measured on the same sample. The information related to the acyl chains is obtained by the shift of a few nanometers to higher values at the phase transition temperature of the frequency corresponding to the symmetric or asymmetric stretching vibrational modes of CH_2 groups [19,20]. In this regard, the shift to higher frequencies of the ν_s CH_2 stretching as a function of the water content has been also reported for DMPC [21].

FTIR spectroscopy is also a valuable tool to obtain molecular information, without adding perturbing probes, of changes in water states by evaluating the position and width of the 3200–3600 nm bands parallel to the changes in the CH_2 region. The broad IR ν_{13} (OH) band, centered at 3400 cm^{-1}, corresponds to several coupled OH vibrational modes: the fundamental symmetrical (ν_1) and antisymmetrical (ν_3) stretching, and the second overtone of the bending (ν_2) vibrational modes [22,23]. In addition, FTIR spectroscopy is especially suitable for identifying H-bonds between interfacial water molecules and phospholipid head groups. Generally speaking, the formation of a H-bonded complex between two atoms A and B, A–H. . .B, leads to a weakening of the A–H bond and, thereby, a downshift of the frequency of the A–H stretching vibration by a few tens of cm^{-1}. The width in frequency of ν_{13} (OH) band reflects the distribution in strength of the H-bonds between phospholipid and interfacial water molecules.

The presence of water beyond the hydration shell of the phospholipid head groups has been described as confined water or water in restricted domains [24]. The properties of these confined regions of water have been ascribed to the influence of the adjacent wall in several materials [25,26]. In the case of lipid membranes, these water molecules are probably confined between hydrocarbon chains, mainly at the first carbon atoms [9]. Water facing apolar regions would be organized in a different H bond array than that bound to polar groups such as CO and PO, and also it would be different from the H bond coordination of pure water. As chain states are different in the gel and the fluid state, it would be reasonable to think that water may organize in a different way when facing membranes in each of these two states. However, a direct measure of the water states in relation with the phase state of the lipid acyl chains has not been so far analyzed.

In this paper, we present a rational description of the water pocket creation and the influence of the adjacent wall formed at the phase transition by analyzing the changes of FTIR/ATR spectra in the regions corresponding to the CH_2 and water band shifts with temperature.

2. Materials and methods

2.1. Materials

1,2-Dioleoyl-sn-glycero-3-phosphocholine (DOPC), 1,2-dimyristoylphosphatidylcholine (DMPC), 1,2-dipalmitoyl-sn-glycero-3-phosphocholine (DPPC) and 1,2-dimyristoylphosphatidylethanolamine (DMPE) were obtained from Avanti Polar Lipids, Inc. (Alabaster, AL). Purity of the lipids was found to be >99% by thin layer chromatography and used without further purification.

2.2. IR spectroscopic measurements of water bands

Samples for infrared spectroscopy were prepared by hydrating 3–5 mg of the dry lipids with 50–70 μL of H_2O at pH 7.4 followed by vigorous vortexing at temperatures well above the gel/liquid crystalline phase transition of the lipid.

After hydration, samples were squeezed between the CaF_2 windows sample cell equipped with a spacer of appropriate thickness. Once the sample was mounted in the holder of the instrument, its temperature was controlled (between −5 and 60 °C) by an external, computer-controlled circulating water bath within ±0.1 °C.

The presence of water in the system was monitored by the saturation of the peak of the ν_{asym} (PO_2^-) band, which shows an absorption peak at 1240 cm^{-1} and shift to 1230 cm^{-1} when lipids are saturated in water.

The spectra were recorded with an FTIR Nicolet TM 380 spectrophotometer, provided with a DTGS detector and a KBr beam splitter. A total of 320 scans were done for a series of hydrated samples with a 2 cm^{-1} resolution. A number of different samples (no less than three) were processed to obtain a standard deviation below the resolution of the equipment.

In the spectral regions of interest, the observed absorption bands are usually the result of the summation of broad overlapping components. In such cases, Fourier deconvolution was used to accurately determine the frequencies of the component bands (band narrowing factors: 1.6–2.2), followed by curve fitting to obtain the band's widths and intensities. Each band was simulated by a Gaussian–Lorentzian function, for which best fit estimates of band shape was achieved with ~70% Gaussian contribution.

The OH stretching band of water is centered at around 3430 cm^{-1} and shifts to higher frequencies when solutes promote non-linear hydrogen bonding and to lower frequencies when stronger H bonding is promoted correlating with increased linear H bonding [27].

2.3. IR spectroscopic measurements of methylene CH stretching bands

The lipid order state and the motional freedom of the methylene groups were monitored by IR spectra of each phospholipid recorded at the 3000–2800 cm^{-1} range in an IFS55 FTIR spectrophotometer (Bruker, Ettlingen, Germany) purged with N_2 as a function of temperature [28].

Fifteen microliters of the liposome samples was deposited under a stream of nitrogen on one side of a trapezoidal germanium ATR plate with an internal reflection element of 52 × 20 × 2 mm with an aperture angle of 45° yielding 25 internal reflections. While evaporating, capillary forces flattened the membranes, which spontaneously formed oriented multilayer arrangements. Under these conditions a well-ordered multilayer stack is formed and remains fully hydrated under a buffer flow [29]. Spectra were recorded with 2 cm^{-1} spectral resolutions with a broad band MCT detector provided by Bruker. A total of 128 scans were averaged for one spectrum at each temperature analyzed. Each spectrum was recorded between 3 and 5 times.

An average at each temperature is plotted with a standard deviation of $\pm 0.2\ cm^{-1}$. The reproducibility of the measurements ($\pm 0.2\ cm^{-1}$) guarantees the significance of the difference of spectra for the different lipids at each temperature. All the software used for data processing was written under MATLAB 7.0 (MathWorks Inc., Natick, MA).

3. Results

Fig. 1 shows the frequency shifts of the symmetric [ν_s CH_2] (panel A) and asymmetric [ν_{as} CH_2] (panel B) stretching mode bands as a function of the reduced temperature for the different lipids assayed. As a result of the comparison, it is observed that in all cases an increase in frequency is noticeable at the phase transition well above the experimental error. Although the 2920 cm^{-1} and 2850 cm^{-1} absorption bands can both be used to monitor hydrocarbon chain melting at the phase transition, the [ν_{as} CH_2] 2920 cm^{-1} band is rarely used in practice. Instead, the [ν_s CH_2] band near 2850 cm^{-1} is usually free of significant overlapping contributions with the CH_3 group vibrational modes. Thus, as long as lipid hydrocarbon chains are the predominant source of CH_2 groups in the sample, the ν_s (CH_2) band can be effectively used for the detection of lipid hydrocarbon chain-melting phase transitions and, to some extent, for semiquantitative characterizations of concomitant changes in hydrocarbon chain conformational disorder [19,21].

The abrupt wavenumber increase for the ν_s (CH_2) [2850.0–2852.5 cm^{-1}] band at the reduced T_c is well above the standard deviation of the average measures and corresponds to a transition to less ordered alkyl chains as reported by other methods. These plots clearly indicate that, although in all lipids an increase in the frequency is observed at the phase transition, the frequency values reached at the liquid crystalline state are not similar for the different lipids. This is better shown in Fig. 2, in which both frequency values at a reduced

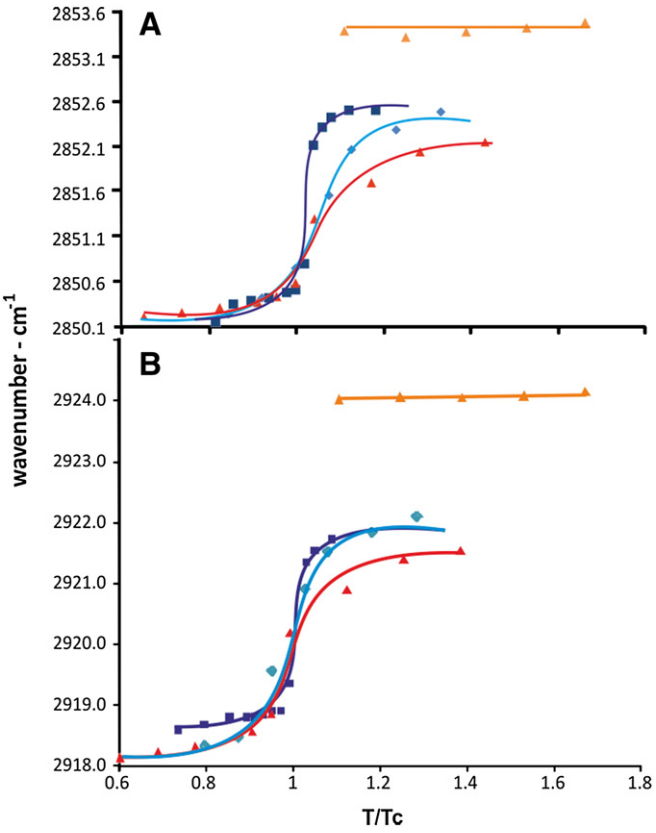

Fig. 1. Changes in the CH_2 methylenes symmetric (A) and asymmetric (B) stretching frequencies as a function of T_r (= T/T_c) for (▲) DMPC, (◆) DPPC, (■) DMPE and (▲) DOPC. The average standard deviation after the analysis of at least different batches was $\pm 0.2\ cm^{-1}$.

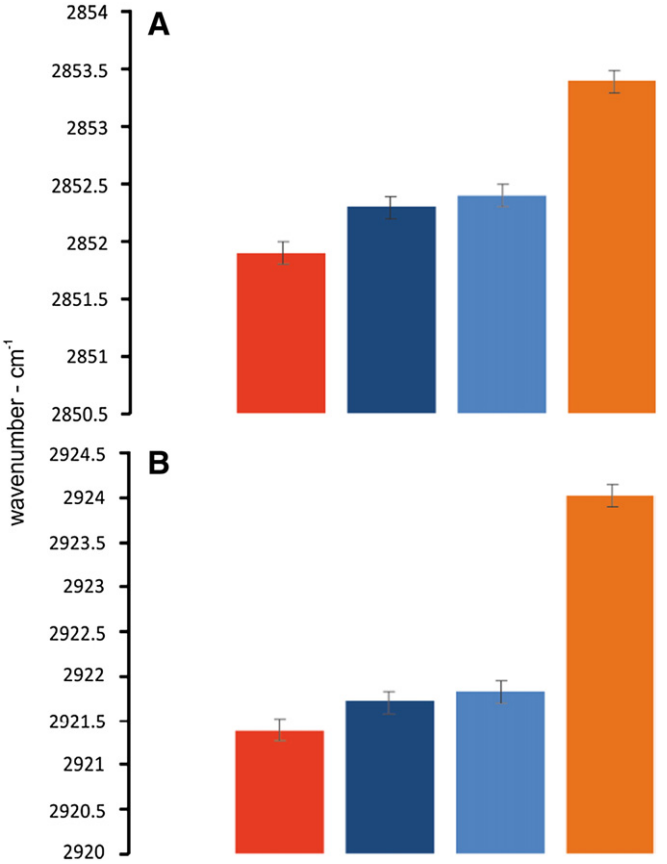

Fig. 2. Frequency values above T_c of the asymmetric (A) and symmetric (B) stretching mode of CH_2 groups for (▲) DMPC, (◆) DPPC, (■) DMPE and (▲) DOPC.

temperature above $T/T_c = 1$ are compared for different lipids. It is clearly shown that the frequency corresponding to the CH_2 groups in DOPC is much higher than those corresponding to fluid DMPC or DPPC. This denotes that fluidity, taken as a macroscopic disordered state of the lipid phase has, at the molecular level, different arrangements according to the lipid composition. While the increase in change length affects slightly the frequency, important changes are observed when an unsaturation is present.

The frequency shift in FTIR can be interpreted in molecular terms, according to the relation between frequency (ν) and force constant (k) of a bond,

$$v = 1/2\prod\sqrt{k/\mu} \quad (1)$$

where μ is the reduced mass of the atoms of the bond. Thus, the shift to higherr frequencies of all lipids, shown in Fig. 1, is related to an increase in the constant force, according to Eq. (1), i.e., a strengthening of the C–H bonds. In the gel state, acyl chains are packed closed to each other and, in consequence, the lateral interactions by dispersion forces between the CH_2 groups of adjacent chains are enhanced. This intermolecular interaction explains why the frequency is lower in the gel than in the fluid state. At the transition temperature, the frequencies of ν_s (CH_2) and ν_{as} CH_2 shift to higher values, denoting that the bond strength increases, which can be ascribed to the reduction of London intermolecular interactions by the increase of interchain distance. Thus, low frequencies for the CH_2 band are due to populations of connected methylene groups, while after the phase transition, the disorder promotes the increase of isolated populations (i.e., non connected CH_2). For this reason, at temperatures above T_c a lipid molecule is very flexible and does not have a defined shape per se. Indeed, under such

conditions its "shape" is better defined as that corresponding to the average volume it occupies while minimizing the packing free energy. To a large extent, this "shape" is determined by the phase state of the lipid aggregate and not the other way around [30]. In other words, average volume is given by spaces occupied by CH_2 residues or empty or vacant spaces.

The derivation of the curves in Fig. 1A denotes different distributions of CH_2 populations around the reduced temperature (Fig. 3). The left-hand wing before the peak indicates that connected population prevails and, vice versa, after the transition the population of isolated groups predominates.

Fig. 3 also denotes that this distribution of connected and isolated CH_2 populations is different depending on the lipid acyl chain and polar head group. For instance, DMPE presents a distribution narrower than DMPC. In contrast, DMPC and DPPC differ between them slightly. The corresponding areas beneath the curves are 3.95, 3.87, and 2.81 for DMPC, DPPC and DMPE, respectively. For the first two lipids, the distributions are rather wide indicating that isolated groups are probably present in the connected (gel) phase and some lipids are clustering in the fluid (isolated residues) state. This is a direct measure of the defects postulated by molecular dynamics [31].

Interestingly, lipids with little changes in its hydration at the phase transition, such as DMPE, show a very narrow distribution indicating that isolated populations only appear very near the transition. In other words, in these lipids, isolated defects are unlikely below the transition temperature and connected clusters are less probable above the phase transition. This behavior is a strong indication that the appearance of isolated CH_2 populations is concomitant with the ability of lipids to incorporate water [24,32,33].

In this regard, the water bands for pure water are modified in the presence of lipids as shown in Fig. 4. The band peak for pure water, centered around 3414.0 cm^{-1}, indicates a wide distribution of H bonds (Fig. 4). When lipids are swollen by heating them above the phase transition and then cooled down to 18 °C, this band shifts to 3447.4 cm^{-1} and two new bands, one around 3200 cm^{-1} and another at 3600 cm^{-1} are apparent (Fig. 4A). Similar patterns were observed for gel DMPE (Fig. 4B).

Deconvolution of water bands allows the distinguishing of several water populations centered around 3590.0 cm^{-1}, 3447.4 cm^{-1}, and 3242 cm^{-1} in the gel state. Similar bands in this range were also reported for cationic lipids [34].

The new band shoulder at 3590.3 cm^{-1} can be assigned to less H bound water molecules due to its comparatively high peak frequency. In addition, the peak at 3241.7 cm^{-1} denotes a population of water molecules with stronger H bonds.

It can be concluded that swollen lipids stabilized in the gel state induce new water populations. These water states apparently are indifferent to the lipid specie since a similar peak distribution is observed for DMPE in the gel sate (Fig. 4B). It must be noticed that in this state the CH_2 populations as denoted in Fig. 1 appears to be similar.

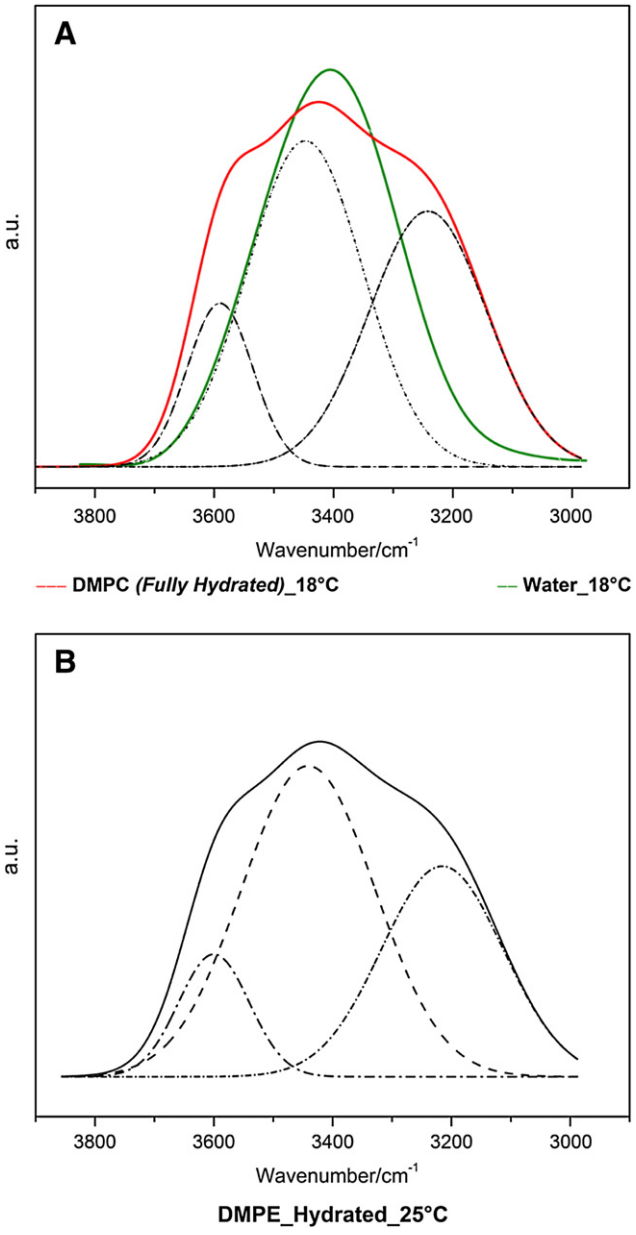

Fig. 4. Water bands for DMPC (——) and water (——) (A) and for DMPE (B) bilayers in the gel state.

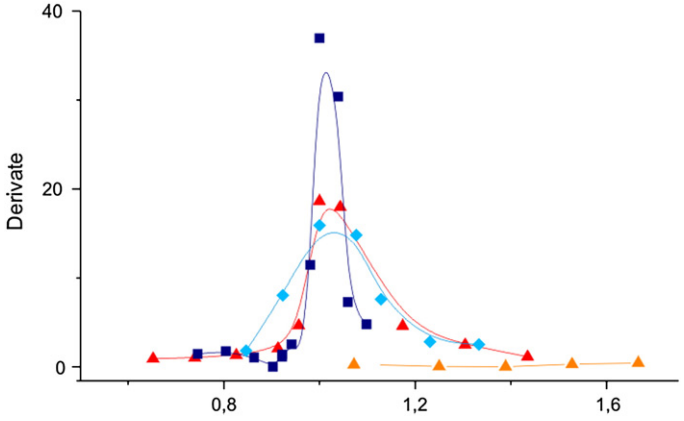

Fig. 3. Derivative of the stretching frequency ($d\nu$ / dT_r) VS T_r for the lipids in Fig. 1. (▲) DMPC, (◆) DPPC, (■) DMPE and (▲) DOPC.

The band at 3400 cm^{-1} region observed in the gel state disappears above the phase transition at the expense of an increase in the bands at 3296.8 cm^{-1} and 3554.2 cm^{-1} regions (Fig. 5A). This suggests that when lipids are in the fluid state, the band of neat water disappears at the expense of those corresponding to highly bound and unbound water species.

Finally, the water bands for DOPC are shown in Fig. 5B. It is observed that these bands are much more superposable with the water band for DMPC in the gel state than for DMPC in the fluid one.

4. Discussion

It is well known that the global cooperativity at the phase transition derived from DSC is usually identified with the rotational isomers of the

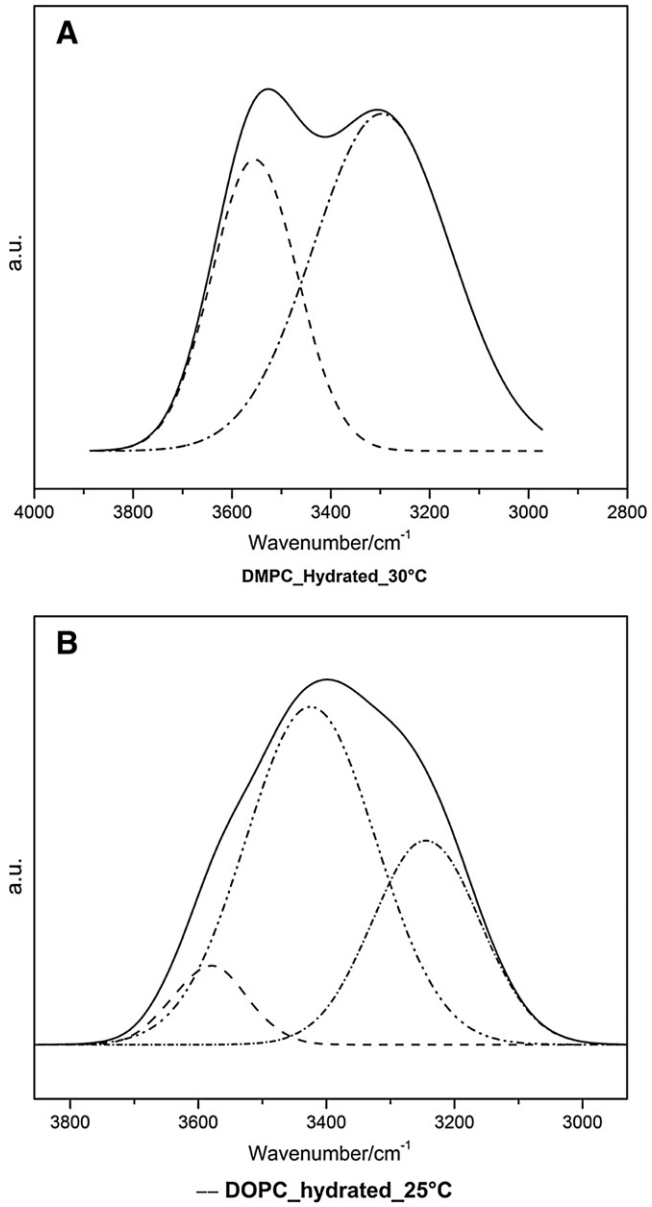

Fig. 5. Water bands for fully hydrated DMPC (A) and DOPC bilayers (B) in the fluid state.

CH_2 residues [12,14]. In this regard, the low ordered state is given by the predominance of a CH_2 isolated population, confirmed by the present FTIR data. Similarly, high order is concomitant with an increase of connected CH_2 groups.

The observation of Figs. 4 and 5 denotes that water structure changes at the phase transition in addition to changes in the membrane state. This decrease in water order at the phase transition is congruent with that previously reported by the calorimetric data of DMPC in D_2O, denoting that a considerable contribution to melting enthalpic change is due to water [35].

In particular, the analysis of the water bands below and above the phase transition temperature of DMPC denotes that the band centered at lower frequencies shifts 55 cm^{-1} to higher frequencies (blue shifts) when going from the gel to the fluid state. At the phase transition, the water band centered at the higher frequency shifts downwards 36 cm^{-1} (red shift). The blue shift would correspond to a weakening of the H bonds and the red shift to its reinforcement. The simultaneous shift of the central pure water population to lower and higher frequencies indicates that in the fluid state water is facing different types of groups exposed to water in the liquid crystalline state. An upward frequency shift of the central band at 3400 cm^{-1} has been reported, although of a lower magnitude, when NaCl was dissolved in water [36], which was attributed to the formation of non linear hydrogen bonds. In the presence of gel lipids this shift can be ascribed to the disruption of the neat water structure near exposed phosphate groups. In the fluid state the blue shift could be explained as a consequence of the higher exposure of the PO and CO groups to water, thus perturbing H bond water network.

On the other hand, the shifts to lower frequencies suggest that H bonds are reinforced in comparison to pure water. This is consistent with water facing non polar walls such as the acyl hydrocarbon chains. Both, acyl chains and head group exposure to water are congruent with the area per lipid increase [11] and hydration increase produced at the gel–fluid phase transition [21].

The results of Figs. 1 and 4 indicate that the changes corresponding to the lateral CH_2 interactions are parallel to a change in the state of water in terms of hydrogen bonding populations. What types of H bonds are concerting water molecules according to the different frequency bands observed?

As reported elsewhere [37,38], the boundary structure greatly influences the structure and dynamics of the water. Specifically, the hydrophobic apolar surfaces slow down the dynamics [36]. In small systems, with dimensions of 3–8 Å, the dynamics are slowed significantly, and the velocity autocorrelation function resembles that of solid ice, i.e., low frequency populations [37]. Histograms of the spatial dependence of the hydrogen-bond lifetimes show confinement or local template environmental ordering, and one can infer that the dynamics are significantly slower near the structured hydrophilic boundary. Local environment indeed affects the structure and dynamics of water. The formation of water tunnels built across an alkane monolayer requires a minimum diameter in order to get filled and the existence of water–water hydrogen bonds, a necessary condition for penetration [27]. From the comparison of the results obtained in the CH_2 region with those of the water bands it is concluded that in the gel state, CH_2 contact (giving place to low frequencies) are concomitant to low H bonded water populations, i.e., small water clusters. Above the phase transition, CH_2 frequency increases denoting isolated populations with an increase in H-bonding in water molecules. Thus, water domains, at least partially organized by H-bonding, are formed in between acyl chains in the fluid state.

The appearance of strong H-bonds between water molecules above the phase transition is consistent with the reinforcement of water structure in the presence of non polar residues such as the CH_2 groups. Water shows a strengthening of the "local tetrahedral" structure while confined template environments are formed due to thermal fluctuations of the acyl chains. For smaller systems, local order is prevalently dominant, and hence, frequency band of the water populations shifts to higher values while the larger systems tend toward bulk-like dynamics. A schematic picture of the state of lipids and water above the phase transition is shown in Fig. 6. Taken together the observation in the CH_2 frequency values and the water bands, the increase in isolated CH_2 populations is congruent with the small nano environments of water structure. This is compatible with the formation of water clustering in between the lipid acyl chains when the bilayer is in the liquid crystalline state [37,38] and also with the appearance of hydrophobic defects at the expense of the disappearance of kinks [39].

As observed in Fig. 2 and from the calculation of the area beneath the curves in Fig. 3, the CH_2 isolated populations are not the same for different lipids although they are in the same state. Specifically, a significant increase in isolated populations is found in DOPC.

It has been reported that the bilayer structure of monounsaturated lipids contains defective, free volume-like places that provide freedom for phospholipid acyl-tail motions at low temperatures as detected by Raman spectroscopy [40]. This void volume in DOPC may confine water in small pools (Fig. 6, right hand) in contrast to the molecularly

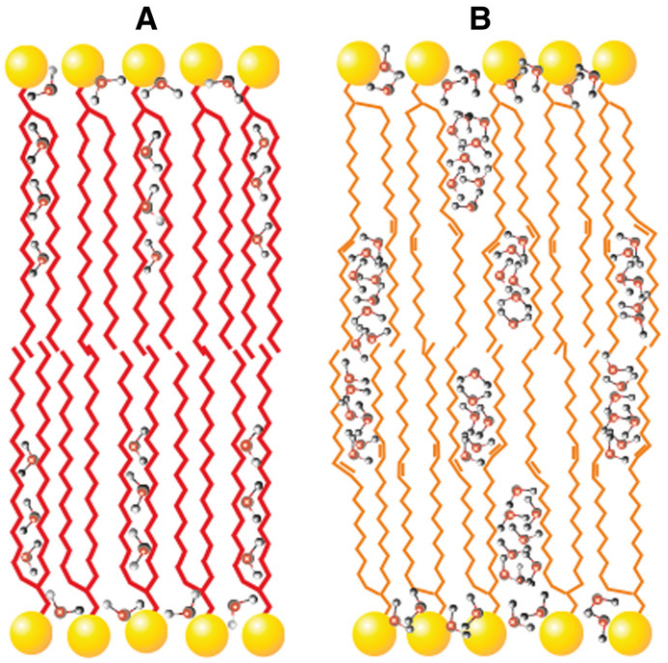

Fig. 6. Schematic representation of lipid and water states for DMPC (A) and DOPC (B) above the phase transition.

dispersed water in kinks formed between saturated chains (Fig. 6, left hand).

Therefore, it would be expected that water species in fluid DOPC be different in comparison to those in fluid DMPC. It is clearly observed in Figs. 4 and 5 that this is the case. Moreover DOPC water band spectra are comparable to those of DMPC in the gel state, i.e., similar to bulk water bands.

In an extension of the kink model [5], the permeation of water-soluble non-electrolytes, such as glycerol, erythritol, urea and others, was explained by the condensation of kinks to form an aqueous space with the size of the permeant solute. In addition, the permeation rate was correlated to the ability of the solute to form hydrogen bonds [41].

The presence of unsaturation in DOPC produces a heterogeneous media in which void spaces would be occupied by water. Thus, in parallel to the increase in isolated populations, the population of bulk water species increases. This is reasonable since pools will include water molecules surrounded by other water molecules far from the surface. The magnitude of the effects of confinement greatly depends on the number of hydrogen bonds available per water as well as the lifetime of nearby hydrogen bonds.

In fluid saturated lipid membranes, molecularly homogeneously dispersed waters are facing hydrophobic residues. In this regard, some considerations about H bonds in water in a CH_2 matrix should be done. H bonds are conventionally defined as the intermolecular interaction of X–H—X were X and Y are atoms of moderate and strong electronegativity [42]. Water may be in contact with the carbonyl groups forming the –C═O–H association or with the methylene groups forming the CH–OH. It has been argued that the last one is rather a contact or and an interaction rather than a bond. This last case is classified as a non-conventional H-bond since the donor atom is not oxygen [43,44].

Recently, reported rotational spectroscopic studies on small dimers and oligomers bound by weak hydrogen bonds show that the driving forces, the spatial arrangement and the dynamical features displayed are very different from those involved in stronger and conventional hydrogen bonds [43]. The very small binding energies (similar to those of van der Waals interactions) imply that networks of weak hydrogen bonds often obtain the stabilization of the dimer. Even in the presence of multiple bonds the partner molecules show a high degree of internal freedom within the complex. Several examples of molecular adducts bound by weak hydrogen bonds formed in free jet expansions were recently characterized by rotational spectroscopy. They include weakly bound complexes of weak donors with strong acceptors (C–H O, N, S–H O, N), strong donors (O–H, N–H) with weak acceptors such as the halogen atoms [45,46].

The hydration of some CH group as in ethers produces a shift to blue and a decrease in the intensity, meaning a decrease in H bonding [47,48]. This is in complete agreement with our analysis of water in the fluid state of saturated acyl chains.

Water molecules in confined pools of few nanometers in diameter or at interfaces undergo hydrogen bond structural dynamics that differ drastically from the dynamics they undergo in bulk water [49]. Orientation motions of water require hydrogen bond network rearrangement [50]. It has also been suggested that reorientation of the O–H vector and hydrogen bonds time correlation is less influenced by hydrophobic groups than hydrophilic groups do [51]. This is somehow related with the idea that interfacial effects may dominate the hydration forces linked to interfacial structural messages [52].

5. Conclusions

Macroscopic disordered state of the lipid phase has, at the molecular level, different arrangements according to the lipid composition.

Changes in the type of water populations are concomitant with the shift of methylene vibrational mode frequencies to higher values.

The increase in isolated populations of methylenes is congruent with the formation of highly ordered water cluster bonded by hydrogen bonds.

This is consistent with the formation of water pockets in nano environments that accumulates free energy. The low entropy of these water arrangements, compensated by the disorder in the acyl chains, can be the thermodynamic driving force for peptide insertion into membranes.

Acknowledgements

This work was supported with funds from Agencia Nacional de Promoción Científica y Tecnológica, PICT (2007 757), CONICET (PIP 5476), and UBACyT (20020090200663).

EAD and MAF are members of the Research Career of CONICET (Consejo Nacional de Investigaciones Científicas y Técnicas de la República Argentina).

AB is a recipient of a post doctoral fellowship of CONICET (Consejo Nacional de Investigaciones Científicas y Técnicas de la República Argentina).

References

[1] L. MacCallum, W.F. Bennett, D.P. Tieleman, Distribution of amino acids in a lipid bilayer from computer simulations, Biophys. J. 94 (2008) 3393–3404.
[2] C. Wimley, S.H. White, Experimentally determined hydrophobicity scale for proteins at membrane interfaces, Nat. Struct. Biol. 3 (1996) 842–848.
[3] J.A. Freites, D.J. Tobias, H.G. von Heijne, S.H. White, Interface connections of a transmembrane voltage sensor, Proc. Natl. Acad. Sci. U.S.A. 102 (2005) 15059–15064.
[4] A.M. Bouchet, F. Lairion, E.A. Disalvo, Role of guanidinium group in the insertion of L-arginine in DMPE and DMPC lipid interphases, Biochim. Biophys. Acta 1798 (2010) 616–623.
[5] H. Träuble, Movement of molecules across lipid membranes: a molecular theory, J. Membr. Biol. 4 (1971) 193–208.
[6] T.H. Haines, L. Liebovitch, A molecular mechanism for the transport of water across phospholipid bilayers, in: E.A. Disalvo, S.A. Simon (Eds.), Permeability and Stability of Lipid Bilayers, CRC Press, Boca Raton, FL, 1995, pp. 126–136.
[7] M. Sovago, E. Vartiainen, M. Bonn, Observation of buried water molecules in phospholipid membranes by surface sum-frequency generation spectroscopy, J. Chem. Phys. 131 (2009) 161107–161111.
[8] S.A. Simon, T.J. McIntosh, Depth of water penetration into lipid bilayers, Methods Enzymol. 127 (1986) 511–521.
[9] S.Y. Bhide, M.L. Berkowitz, Structure and dynamics of water at the interface with phospholipid bilayers, J. Chem. Phys. 123 (2005) 224702–224718.

[10] H. Almaleck, G.J. Gordillo, E.A. Disalvo, Water defects induced by expansion and electrical fields in DMPC and DMPE monolayers: contribution of hydration and confined water, Colloids Surf. B, Biointerfaces 102 (2013) 871–878, http://dx.doi.org/10.1016/j.colsurfb.2012.09.031.
[11] J.F. Nagle, S. Tristram-Nagle, Structure of lipid bilayers, Biochim. Biophys. Acta 1469 (2000) 159–195.
[12] D. Marsh, Structural and thermodynamic determinants of chain-melting transition temperatures for phospholipid and glycolipids membranes, Biochim. Biophys. Acta Biomembr. 1798 (2010) 40–51.
[13] G. Cevc, How membrane chain melting properties are regulated by polar surface of lipid bilayer, Biochemistry 26 (1987) 6305–6310.
[14] H. Heerklotz, R.M. Epand, The enthalpy of acyl chain packing and the apparent water-accessible apolar surface area of phospholipids, Biophys. J. 80 (2001) 271–279.
[15] R.C. MacDonald, S.A. Simon, Lipid monolayer states and their relationships to bilayers, Proc. Natl. Acad. Sci. U.S.A. 84 (1987) 4089–4093.
[16] E.A. Disalvo, Optical properties of lipid dispersions induced by permeant molecules, Chem. Phys. Lipids 59 (1991) 199–206.
[17] L.I. Viera, E.A. Disalvo, Optical changes of liposome dispersions and its correlation with the interlamellar distance and solute interaction, Chem. Phys. Lipids 81 (1996) 25–54.
[18] T. Parasassi, G. De Stasio, G. Ravagnan, R.M. Rusch, E. Gratton, Quantitation of lipid phases in phospholipid vesicles by the generalized polarization of Laurdan fluorescence, Biophys. J. 60 (1991) 179–189.
[19] H. Binder, G. Lindblom, A molecular view on the interaction of the Trojan peptide penetratin with the polar interface of lipid bilayers, Biophys. J. 87 (2004) 332–343.
[20] R.N.A.H. Lewis, R.N. McElhaney, Fourier transform infrared spectroscopy in the study of hydrated lipids and lipid bilayer membranes in infrared spectroscopy of biomolecules, in: H.H. Mantsch, D. Chapman (Eds.), Wiley-Liss, NY, 1996, pp. 159–202.
[21] D.R. Gauger, C. Selle, H. Fritzsche, W. Pohle, Chain-length dependence of the hydration properties of saturated phosphatidylcholines as revealed by FTIR spectroscopy, J. Mol. Struct. 565–566 (2001) 25–29.
[22] H. Binder, Water near lipid membranes as seen by infrared spectroscopy, Eur. Biophys. J. 36 (2007) 265–279.
[23] Z. Arsov, M. Rappolt, J. Grdadolnik, Weakened hydrogen bonds in water confined between lipid bilayers: the existence of a long-range attractive hydration force, Chem. Phys. Chem. 10 (2009) 1438–1441.
[24] E.A. Disalvo, F. Lairion, F. Martini, E. Tymczyszyn, M. Frías, H. Almaleck, G.J. Gordillo, Structural and functional properties of hydration and confined water in membrane interfaces, Biochim. Biophys. Acta 1778 (2008) 2655–2670.
[25] P. Lam, K.J. Wynne, G.E. Wnek, Surface-tension-confined microfluidics, Langmuir 18 (2002) 948–951.
[26] N. Giovambattista, P.J. Rossky, P.G. Debenedetti, Effect of pressure on the phase behavior and structure of water confined between nanoscale hydrophobic and hydrophilic plates, Phys. J. E. 73 (4 Pt 1) (2006) 041604.
[27] E.P. Schulz, L.M. Alarcon, G.A. Appignanesi, Behavior of water in contact with model hydrophobic cavities and tunnels and carbon nanotubes Eur, Phys. J. E. 34 (2011) 114–120.
[28] C. Vigano, L. Manciu, F. Buyse, E. Goormaghtigh, J.M. Ruysschaert, Attenuated total reflection IR spectroscopy as a tool to investigate the structure, orientation and tertiary structure changes in peptides and membrane proteins, Biopolymers 55 (5) (2000) 373–380.
[29] F. Scheirlinckx, V. Raussens, J.M. Ruysschaert, E. Goormaghtigh, Conformational changes in gastric H^+/K^+-ATPase monitored by difference Fourier-transform infrared spectroscopy and hydrogen/deuterium exchange, Biochem. J. 382 (Pt 1) (2004) 121–129.
[30] K.A. Sharp, J.N. Vanderkooi, Water in the half shell: structure of water, focusing on angular structure and solvation, Acc. Chem. Res. 43 (2010) 231–239.
[31] O.G. Mouritsen, Theoretical models of phospholipid phase transitions, Chem. Phys. Lipids 57 (2–3) (1991) 179–194.
[32] H.L. Casal, H.H. Mantsch, Polymorphic phase behaviour of phospholipid membranes studied by infrared spectroscopy, Biochim. Biophys. Acta 779 (4) (1984) 381–401.
[33] A.M. Bouchet, M.A. Frías, F. Lairion, F. Martini, H. Almaleck, G. Gordillo, E.A. Disalvo, Structural and dynamical surface properties of phosphatidylethanolamine containing membranes, Biochim. Biophys. Acta Biomembr. 1788 (2009) 918–925.
[34] L. Woiterski, D.W. Britt, J.A. Käs, C. Selle, Oriented confined water induced by cationic lipids, Langmuir 28 (2012) 4712–4722.
[35] Chang-Hwei Chen, Interactions of lipid vesicles with solvent in heavy and light water, J. Phys. Chem. 86 (1982) 3559–3562.
[36] S. Romero-Vargas Castrillon, N. Giovambattista, I.A. Aksay, P.G. Debenedetti, Effect of surface polarity on the structure and dynamics of water in nanoscale confinement, J. Phys. Chem. B 113 (2009) 1438–1446.
[37] J. Goldsmith, C.C. Martens, Effect of boundary conditions on the structure and dynamics of nanoscale confined water, J. Phys. Chem. A 113 (2009) 2046–2052.
[38] M.F. Chaplin, A proposal for structuring of water, Biophys. Chem. 83 (1999) 211–221.
[39] S.J. Marrink, D.P. Tieleman, A.R. van Buuren, H.J.C. Berendsen, Membranes and water — an interesting relationship, Faraday Discuss. 103 (1996) 191–201.
[40] N.V. Surovtsev, N.V. Ivanisenko, K.Yu. Kirillov, S.A. Dzuba, Low-temperature dynamical and structural properties of saturated and monounsaturated phospholipid bilayers revealed by Raman and spin-label EPR spectroscopy, J. Phys. Chem. B 116 (2012) 8139–8144.
[41] E.A. Disalvo, Permeation of water and polar solutes in lipid bilayers, Adv. Colloid Interface Sci. 29 (1988) 141–170.
[42] G.C. Pimentel, A.L. McClellan, The Hydrogen Bond, W. H. Freeman and Company, San Francisco and London, 1960.
[43] S. Melandri, Union is strength: how weak hydrogen bonds become stronger, Phys. Chem. Chem. Phys. 13 (2011) 13901–13911.
[44] M. Nishio, The CH/π hydrogen bond in chemistry. Conformation, supramolecules, optical resolution and interactions involving carbohydrates, Phys. Chem. Chem. Phys. 13 (2011) 13873–13900.
[45] S. Scheiner, Comparisons of CH···O to NH···O in proteins and PH···N to direct P···N interactions, Phys. Chem. Chem. Phys. 13 (2011) 13860–13872.
[46] W.A. Herrebout, M.A. Suhm, Weak hydrogen bonds — strong effects? Phys. Chem. Chem. Phys. 13 (2011) 13858–13859.
[47] J. Jorly, D.J. Eluvathingal, Red-, blue-, or no-shift in hydrogen bonds: a unified explanation, J. Am. Chem. Soc. 129 (2007) 4620–4632.
[48] B.J. van der Veken, W.A. Herrebout, R. Szostak, D.N. Shchepkin, Z. Havlas, P. Hobza, The nature of improper, blue-shifting hydrogen bonding verified experimentally, J. Am. Chem. Soc. 123 (2001) 12290–12293.
[49] M.D. Fayer, N.E. Levinger, Analysis of water in confined geometries and at interfaces, Annu. Rev. Anal. Chem. 3 (2010) 89–107.
[50] D. Laage, G. Stirnemann, J.T. Hynes, Why water reorientation slows without iceberg formation around hydrophobic solutes, J. Phys. Chem. B 113 (2009) 2428–2435.
[51] J. Chowdhary, B. Ladanyi, Hydrogen bond dynamics at the water/hydrocarbon interface, J. Phys. Chem. B 113 (2009) 4045–4053.
[52] G. Cevc, Hydration force and the interfacial structure of the polar surface, J. Chem. Soc. Faraday Trans. 87 (1991) 2733–2739.